

A search for $J^{PC} = 1^{-+}$ exotic mesons in the $\pi^{-}\pi^{-}\pi^{+}$ and $\pi^{-}\pi^{0}\pi^{0}$ systems

A. R. Dzierba, R. Mitchell, A. P. Szczepaniak,* M. Swat, and S. Teige
 Department of Physics, Indiana University, Bloomington, IN 47405.

(Dated: November 19, 2017)

A partial wave analysis (PWA) of the $\pi^{-}\pi^{-}\pi^{+}$ and $\pi^{-}\pi^{0}\pi^{0}$ systems produced in the reaction $\pi^{-}p \rightarrow (3\pi)^{-}p$ at 18 GeV/c was carried out using an *isobar* model assumption. This analysis is based on 3.0M $\pi^{-}\pi^{0}\pi^{0}$ events and 2.6M $\pi^{-}\pi^{-}\pi^{+}$ events and shows production of the $a_2(1320)$, $\pi_2(1670)$ and $\pi(1800)$ mesons. An earlier analysis of 250K $\pi^{-}\pi^{-}\pi^{+}$ events from the same experiment showed possible evidence for a $J^{PC} = 1^{-+}$ exotic meson with a mass of 1.6 GeV/c² decaying into $\rho\pi$. In this analysis of a higher statistics sample of the $(3\pi)^{-}$ system in two charged modes we find no evidence of an exotic meson.

PACS numbers: 11.80.Cr, 13.60.Le, 13.60Rj

Keywords: meson resonances

Quantum chromodynamics (QCD) predicts a spectrum of *hybrid* mesons beyond the $q\bar{q}$ bound states of the conventional quark model in which the gluons binding the quarks manifest their degrees of freedom. Lattice QCD and QCD-inspired models predict that the gluonic field within the meson forms a flux tube for quark separation greater than 1 fermi [1]. When the flux tube is in its ground state conventional mesons emerge. When the flux-tube is in its excited states hybrid mesons emerge. For conventional mesons the spin (J), parity (P) and charge conjugation (C) quantum numbers of the $q\bar{q}$ system are those of a fermion-antifermion system: $\vec{J} = \vec{L} + \vec{S}$ where \vec{L} is the angular momentum between the quarks and \vec{S} is the total quark spin; $P = (-1)^{L+1}$; and $C = (-1)^{L+S}$. Thus $J^{PC} = 0^{++}, 1^{-+}, 2^{+-}, \dots$ are not allowed. These *exotic* quantum numbers are allowed when the quantum numbers of the excited flux-tube are included and are thus a signature for hybrid mesons. The fundamental interest in the spectrum and other properties (decay modes and widths) of hybrid mesons is that flux tubes are thought to be responsible for the confinement of quarks and gluons in QCD.

In 1998, the E852 collaboration reported evidence for the $\pi_1(1600)$, a $J^{PC} = 1^{-+}$ exotic hybrid meson with a mass of 1.6 GeV/c² decaying into $\rho\pi$. The original publication [2] of this result was followed by another [3] giving more details of the analysis based on 250,000 events of the reaction $\pi^{-}p \rightarrow \pi^{-}\pi^{-}\pi^{+}p$ at 18 GeV/c collected in the E852 experiment at Brookhaven Lab in 1994. A search for this state by the VES collaboration in the reaction $\pi^{-}A \rightarrow \pi^{-}\pi^{-}\pi^{+}A$ interactions at 37 GeV/c [4] did not confirm this state. The partial wave analysis (PWA) procedure used to extract these results was based on the *isobar* model assumption whereby the final state 3π system is reached via an intermediate state of a di-pion resonance (*e.g.* σ , $f_0(980)$, $\rho(770)$, $f_2(1275)$, $\rho_3(1690)$) and a bachelor π .

This paper reports on the analysis of additional data collected in 1995 including 3.0M events of the reaction $\pi^{-}p \rightarrow \pi^{-}\pi^{0}\pi^{0}p$ and 2.6M events of the reaction

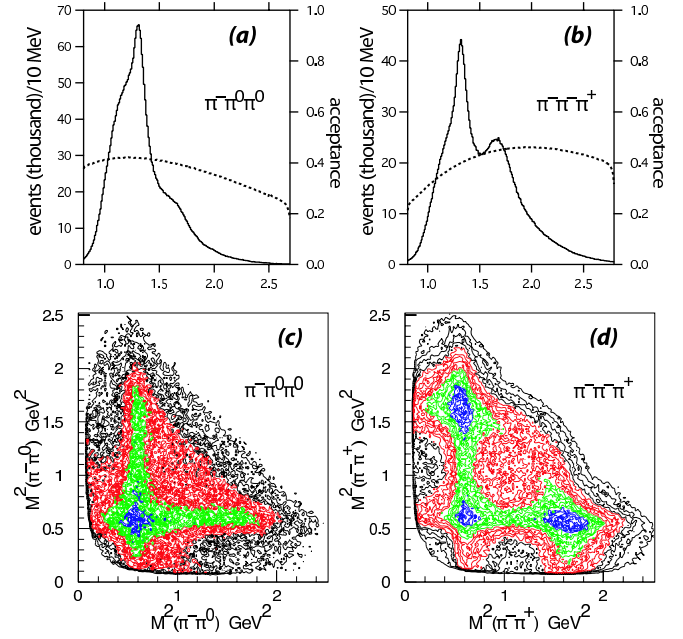


FIG. 1: Acceptance-uncorrected (a) $\pi^{-}\pi^{0}\pi^{0}$ and (b) $\pi^{-}\pi^{-}\pi^{+}$ effective mass distributions along with acceptance functions and the (c) $\pi^{-}\pi^{0}\pi^{0}$ and (d) $\pi^{-}\pi^{-}\pi^{+}$ Dalitz plots for events in the $\pi_2(1670)$ mass region.

$\pi^{-}p \rightarrow \pi^{-}\pi^{-}\pi^{+}p$. We compare the isobar model PWA of these two large data sets with each other and with the analysis presented in [2, 3]. The comparison of the two $(3\pi)^{-}$ modes provides powerful cross checks. Any resonance decaying to $(\rho\pi)^{-}$ should decay equally to $\rho^{-}\pi^{0} \rightarrow (\pi^{-}\pi^{0})\pi^{0}$ and $\rho^{0}\pi^{-} \rightarrow (\pi^{+}\pi^{-})\pi^{-}$ and thus appear with equal probabilities in the two modes. Similarly, any resonance decay to $f_2\pi^{-}$ ought to appear twice as often in $(\pi^{+}\pi^{-})\pi^{-}$ as $(\pi^{0}\pi^{0})\pi^{-}$. And these same isospin rules dictate relationships between the two modes for all other decay sequences. Since the $\pi^{-}\pi^{-}\pi^{+}$ and $\pi^{-}\pi^{0}\pi^{0}$ modes rely on different elements of the detector, any misunderstandings in the acceptance would affect the two modes differently and inconsistencies would result. As

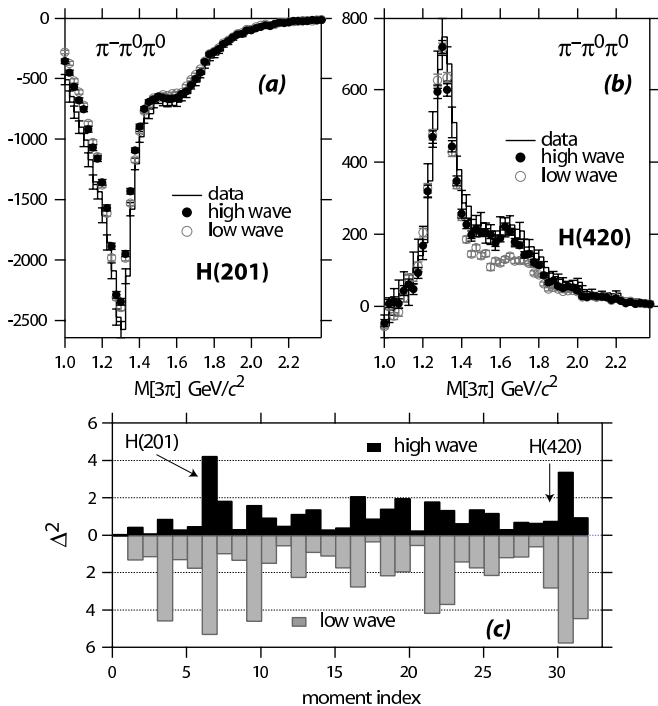


FIG. 2: Comparison of the (a) H(201) and (b) H(420) moments as computed directly from data and from PWA fits for the low and high wave sets for the $\pi^-\pi^0\pi^0$ channel. In (c) the Δ^2 (differences squared divided by errors squared summed over all mass bins and divided by the number of mass bins) for various moments.

the results will show, this is not the case.

The data reported on in this paper were collected in the E852 experiment at the Alternating Gradient Synchrotron (AGS) at Brookhaven Laboratory (BNL) using the multi-particle spectrometer (MPS) augmented with a forward electromagnetic calorimeter (LGD) consisting of 3000 lead glass blocks. An 18.3 GeV/c π^- beam was incident on a liquid hydrogen target. Details about the E852 experiment are given elsewhere [5, 6].

The 1995 run of E852 collected approximately 146M (265M) triggers requiring one (three) forward going charged particles. For those triggers requiring only one forward track, it was also required that the trigger processor [6] detected an energy deposition pattern in the LGD consistent with an effective mass greater than a single π^0 . The kinematic fitting program SQUAW [7] was used in identifying approximately 73M (79M) reconstructed events that were consistent with the topology $\pi^-p \rightarrow (3\pi)^-p$. This constrained fit used the measured track and beam momenta, the measurements from the LGD and constraints on the recoil particle mass ($= m_p$) and di-photon effective masses (two pairs $= m_\pi$) to refine the measured final state particle 4-momenta. In the $\pi^-\pi^0\pi^0$ topology, 13.8M events survived this selection while 16.8M events of the $\pi^-\pi^-\pi^+$ topology survived. Further cuts on fit confidence level, vertex position and

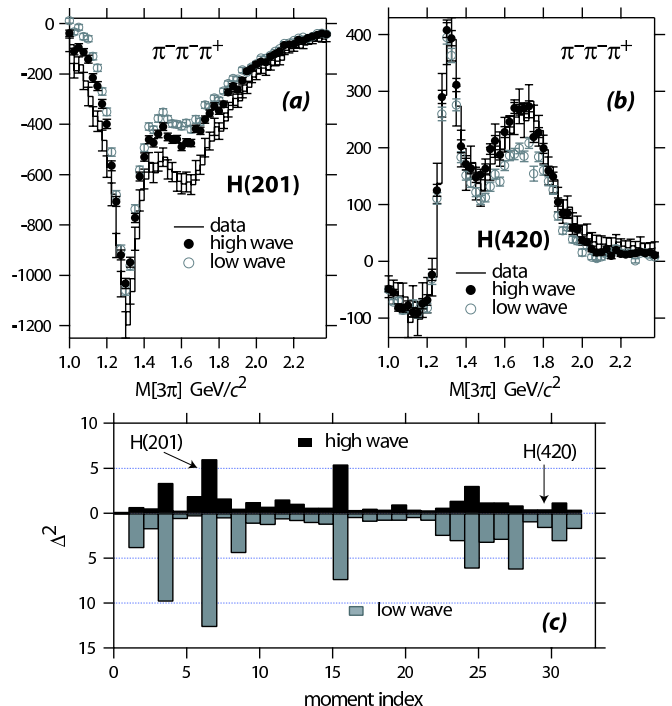


FIG. 3: Comparison of the (a) H(201) and (b) H(420) moments as computed directly from data and from PWA fits for the low and high wave sets for the $\pi^-\pi^-\pi^+$ channel. In (c) the Δ^2 (differences squared divided by errors squared summed over all mass bins and divided by the number of mass bins) for various moments.

correlation between the 3π system and a recoil track produced the final data set analyzed here: 3,025,980 $\pi^-\pi^0\pi^0$ events and 2,585,852 $\pi^-\pi^-\pi^+$ events.

Figures 1 (a) and (b) show the acceptance uncorrected $\pi^-\pi^0\pi^0$ and $\pi^-\pi^-\pi^+$ effective mass distributions respectively. Enhancements in the $a_1(1260)$, $a_2(1320)$ and $\pi_2(1670)$ mass regions are observed. The acceptance in 3π effective mass is also shown in Figures 1 (a) and (b). Dalitz plots for the $\pi^-\pi^0\pi^0$ and $\pi^-\pi^-\pi^+$ systems in the $\pi_2(1670)$ mass region are shown in Figures 1 (c) and (d) respectively. These Dalitz plots clearly show rich structure and bands corresponding to decays into $\pi\rho(770)$ and $\pi f_2(1275)$, motivating application of the isobar model.

The PWA software used in this analysis consisted of programs developed at BNL and Indiana University (IU) [8]. The formalism is similar to that used in [2, 3] but the details of handling the data and doing the the PWA fits differ. The IU software was optimized for running on a 200-processor computer cluster (AVIDD) [9] allowing systematic studies involving many PWA fits, varying isobar parameters and using different wave sets. Results from the two programs were compared with each other and found to be consistent. The IU programs were also used to analyze the data presented in [2, 3] and produced consistent results.

The analysis is performed in the Gottfried-Jackson

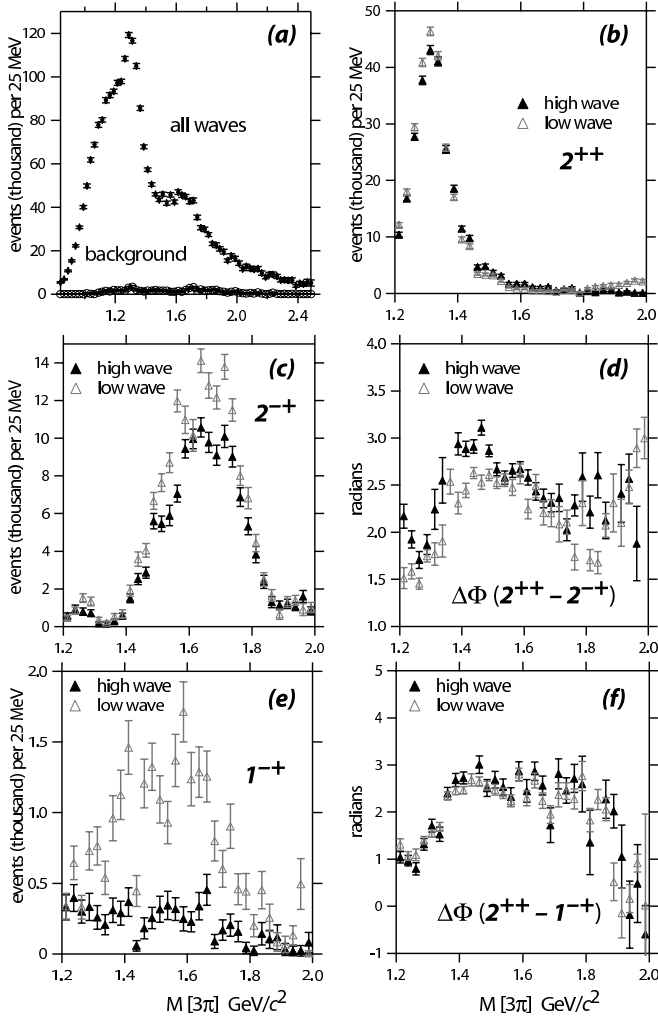


FIG. 4: PWA results for the $\pi^-\pi^0\pi^0$ channel as a function of 3π effective mass: (a) sum of all waves and the background wave; (b) 2^{++} wave; (c) 2^{-+} wave; (d) $\Delta\Phi(2^{++} - 2^{-+})$; (e) 1^{-+} wave; (f) $\Delta\Phi(2^{++} - 1^{-+})$. For (b) through (f) the results for the low wave and high wave sets are shown.

frame. Within the isobar formalism each partial wave is characterized by $J^{PC}M^\epsilon$, (SL), where J , P and C are the spin, parity and charge conjugation of the 3π system, respectively, M is the spin projection along the z axis and ϵ represents symmetry of the 3π system under reflection in the production plane. Finally S is the spin of the isobar and L is the relative orbital angular momentum between the isobar and the bachelor π . Except for the $S = 0$ wave, all $\pi\pi$ resonances are parametrized using relativistic Breit-Wigner functions with Blatt-Weisskopf factors.

Following [10] a sufficient set of partial waves was determined by sequentially removing waves from a parent set containing waves with $J \leq 4$, $M \leq 1$ and $S \leq 3$ and examining the resulting change in likelihood. If no significant change in likelihood was obtained, the wave was removed. The exotic 1^{-+} partial waves were kept even

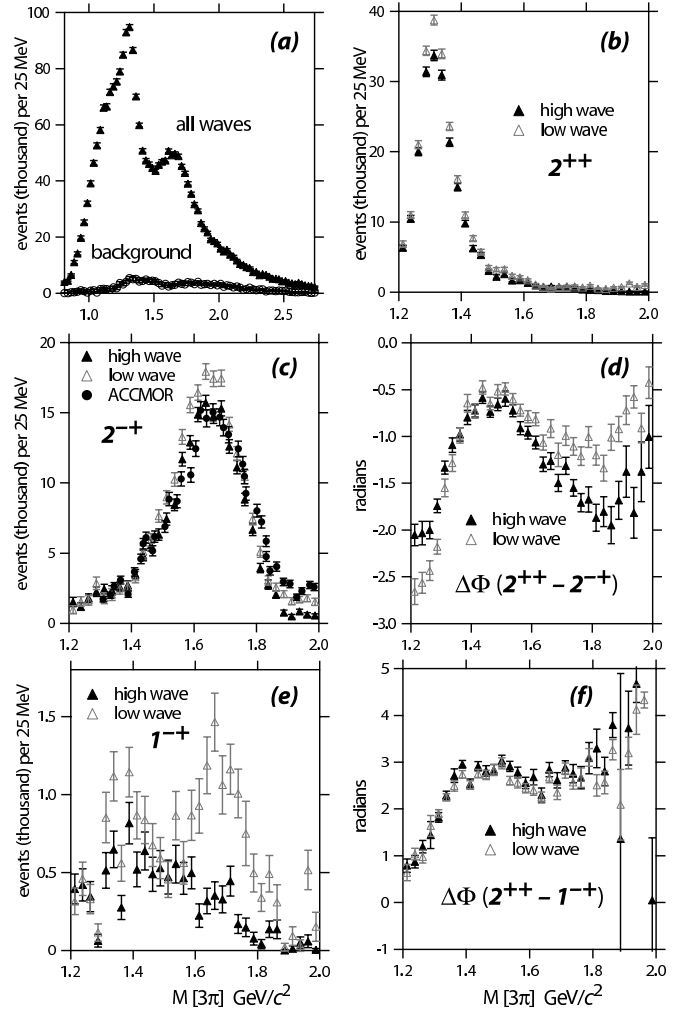


FIG. 5: PWA results for the $\pi^-\pi^-\pi^+$ channel as a function of 3π effective mass: (a) sum of all waves and the background wave; (b) 2^{++} wave; (c) 2^{-+} wave; (d) $\Delta\Phi(2^{++} - 2^{-+})$; (e) 1^{-+} wave; (f) $\Delta\Phi(2^{++} - 1^{-+})$. For (b) through (f) the results for the low wave and high wave sets are shown.

though they would have been chosen for removal by the above criteria – the existence of signals in these waves is discussed below. Based on these criteria the compiled set includes 35 waves and a background wave – we refer to this as the *high wave* set. In comparison, the wave set used in the analysis described in [3] included 20 waves and a background wave – we refer to this as the *low wave* set. The 35 wave set included three additional 1^{++} , seven additional 2^{-+} and seven additional $J \geq 3$ waves. This high wave set did not include two negative reflectivity partial waves ($1^{++}1^-$, (10) and $2^{-+}1^-$, (20)) that were included in the low wave set PWA.

Another arbiter of wave set sufficiency is the comparison of moments, $H(LMN)$, of the $D_{MN}^L(\Omega)$ functions as calculated directly from the data and as calculated using the results of PWA fits. We define $H(LMN) = \int I(\Omega) D_{MN}^L(\Omega) d\Omega$ where Ω represents the Euler angles

of the 3π system [11] and the intensity $I(\Omega)$ is determined directly from experiment or computed using the results of the PWA fits. In Figure 2 we show the H(201) and H(420) moment comparisons as a function of 3π mass for the $\pi^-\pi^0\pi^0$ channel for low wave and high wave set PWA fits. We also show the difference between data and PWA calculations of the moments as Δ^2 (summing differences squared divided by errors squared summed over all mass bins and divided by the number of mass bins) for various moments. Similar plots are shown in Figure 3 for the $\pi^-\pi^-\pi^+$ channel. The moments calculated using the PWA results from the high wave set have better agreement with experimental moments. But there are moments (such as H(201) - shown in part (a) of Figure 3) for which agreement is not achieved and this is most likely due to the inherent inadequacy of the isobar model in describing the underlying production mechanism.

Figures 4 and 5 show the PWA fit results for the $\pi^-\pi^0\pi^0$ and $\pi^-\pi^-\pi^+$ channels respectively as a function of the 3π effective mass. In part(a) of each figure the sum of the waves is shown along with the background wave. The background wave is added incoherently with the other waves and is isotropic in all decay angles. The fitting procedure constrains the sum of all waves to describe the observed 3π effective mass. Parts (b), (c) and (d) of each figure show the mass dependence of the $2^{++}1^+$, (12) and $2^{-+}0^+$, (20) waves and their phase difference. Results are shown for both the low wave and high wave set. To within 10% the acceptance corrected yields of a_2^- in the two 3π modes are equal, consistent with expected decays into $\rho^-\pi^0$ and $\rho^0\pi^-$. And the yield for π_2^- is higher by a factor of two for the $f_2(1275)\pi^-$ modes when $f_2 \rightarrow \pi^+\pi^-$ compared to $f_2 \rightarrow \pi^0\pi^0$, consistent with expectations from isospin. The 2^{++} and 2^{-+} waves and their phase difference are consistent with two interfering Breit-Wigner line shapes. For the 2^{-+} wave in the $\pi^-\pi^-\pi^+$ channel (Figure 5(c)) we also show the published 2^{-+} wave from the PWA of diffractive 3π production in π^-p interactions at 63 and 94 GeV/c from the ACCMOR collaboration [10].

The $1^{-+}1^+$, (11) wave and its interference with the 2^{++} wave are shown in parts (e) and (f) of each figure. When the low wave set is used in the fit, an enhancement is observed for the exotic 1^{-+} wave in the 3π mass region around 1.6 GeV/c², consistent with the observation of [2, 3] - *i.e.* we obtain the same results when we use the same wave set. But the enhancement disappears when the high wave set is used. This effect is observed for both 3π channels. And the phase (see part (d)) of the exotic wave relative to the dominant 2^{++} wave is similar for both wave sets and dominated by the phase of the $a_2(1320)$. The amplitudes of the negative reflectivity exotic waves show the same behavior, disappearing as the fit improves.

The masses and widths of the ρ and the $f_2(1275)$ were varied and the maximum likelihood was achieved using current best values for these quantities [12]. Different parameterizations of the $\pi\pi$ S-wave were also examined [3, 13, 14]. While small changes in the likelihood were observed, no systematic changes in the PWA results occurred.

The PWA results presented here were for data with $0.18 < |t| < 0.23$ (GeV/c)² where t is the square of the momentum transferred from the incoming π^- to the outgoing $(3\pi)^-$ system. PWA fits were also carried out for 12 other regions in t and the results are similar to those presented here.

In summary, there is no evidence for an exotic $J^{PC} = 1^{-+}$ meson in the 3π system and in particular for the $\pi_1(1600)$.

ACKNOWLEDGMENTS

This work was supported by grants from the United States Department of Energy (DE-FG-91ER40661/Task D and DE-FG0287ER40365) and the National Science Foundation (EIA-0116050) for AVIDD.

-
- * Also with the Nuclear Theory Center, Indiana University
- [1] K. J. Juge, J. Kuti and C. Morningstar, hep-lat/0401032 (2004).
 - [2] G. S. Adams *et al.* Phys. Rev. Lett. **81**, 5760 (1998).
 - [3] S. U. Chung *et al.* Phys. Rev. **D65**, 072001 (2002).
 - [4] I. Kachaev *et al.*, hep-ex/0111067 (2001).
 - [5] T. Adams *et al.*, Nucl. Inst. & Meth. **A368**, 617 (1996); Z. Bar-yam *et al.*, Nucl. Inst. & Meth. **A386** 235 (1997); and S. Teige *et al.*, Phys. Rev. **D59**, 012001 (1999)
 - [6] B. B. Brabson *et al.*, Nucl. Inst. & Meth. **A332** 419 (1993); R. R. Crittenden *et al.*, Nucl. Inst. & Meth. **A387**, 377 (1997); J. Gunter, Ph. D. Thesis, Indiana University (1997); and R. Lindenbusch, Ph. D. Thesis, Indiana University (1997).
 - [7] O. Dahl *et al.*, SQUAW kinematic fitting program, Group A programming note P-126, U. California Berkeley (1968).
 - [8] Details about the IU software and PWA can be found at the website: dustbunny.physics.indiana.edu/3p-paper.
 - [9] AVIDD (Analysis and Visualization of Instrument Driven Data) Website: kb.indiana.edu/data/almb.ose.help.
 - [10] C. Daum *et al.* (ACCMOR Collaboration), Nucl. Phys., **B182**,269 (1981).
 - [11] G. Ascoli and H. W. Wyld, Phys. Rev. **D12**, 43 (1975).
 - [12] S. Eidelman *et al.*, Phys. Lett. **B592**, 1 (2004).
 - [13] K. L. Au, D. Morgan and M. R. Pennington, Phys. Rev. **D35**, 1633 (1987).
 - [14] J. A. Oller and E. Oset, Phys. Rev. **D60**, 074023 (1999).